Large-Scale Structure in a Supersonic Slot-Injected Flowfield

R. L. Clark Jr.,* W. F. Ng,† D. A. Walker,‡ and J. A. Schetz§
Virginia Polytechnic Institute and State University, Blacksburg, Virginia

Experimental results that show the existence of organized structures in a high-speed shear-layer flow are presented. Results were obtained using a parallel-array, dual-wire probe in a shear layer created by the mixing of tangential slot injection of supersonic air (M_j = 1.7) into a supersonic air mainstream (M = 3). The slot-injected flowfield was studied at three streamwise locations (X/H of 4, 10, 20). At each station, a region ($1.5 > Y/H > 0.7$) dominated by the upstream boundary layer resulted in structure angles on the order of 50 deg. Structures in this region appeared to be the remnants of structures observed in the upstream boundary layer. Integral length scale in this region was on the order of 3 mm or less and increased to 4 mm at X/H of 20. The effect of a shock impingement upon the shear layer was also investigated. The oblique shock had a nominal pressure ratio of 1.82. Structure angles and integral length scales appeared unaffected by the streamwise pressure gradient caused by the shock impingement.

Nomenclature

H = slot height (1.27 cm)
M = Mach number
t = time
U = local mean velocity
U_∞ = freestream velocity in tunnel
w = wire separation distance (1.33 mm)
X = streamwise position referenced from the exit of slot injection
Y = vertical position referenced from the upper side of the splitter plate or from the floor of the test section
δ = boundary layer thickness
θ = average structure angle
τ = time delay between hot-wire signals as determined from their cross-correlation function

Subscripts

e = tunnel freestream
j = slot injection freestream

Introduction

CURRENT interest in developing an air breathing hypersonic vehicle with supersonic combustion has prompted research in studying the effects of supersonic slot injection into a supersonic flow.[1] In Ref. 1, tangential slot injection of supersonic air (M_j = 1.70) into a supersonic air freestream (M = 3) was investigated. Steady-state measurements and turbulent mass-flux intensity were documented. The present paper is an extension of Ref. 1. The specific thrust of the research reported in this paper was to study the characteristics of organized structures throughout such a flowfield. In the last several years, much research has been dedicated to the study of turbulent structure. Recent studies indicate the existence of a complex deterministic hierarchy of structures.[2]

Studies of organized structures in turbulent boundary layers first began in 1967 when Kline proposed the bursting cycle.[3] Kline then proposed that the bursting phenomenon stimulated the production of turbulent energy and controlled the diffusion of this energy from the inner to the outer layer. Later work by Corino and Brodkey[4] indicated that the bursts accounted for approximately 70% of the Reynolds stress level in the boundary layer near the wall. Kim et al.[5] later showed that the majority of the net production of turbulent kinetic energy in the range of $0 < y^+ < 100$ occurred during bursts. As a result, interest developed in the interaction between the inner and outer layer structures and the large-scale, outer-layer structure of the boundary layer. Studies by Brown and Thomas,[6] Chen and Blackwelder,[7] Moin and Kim,[8] Thomas and Bull,[9] Rajagopalan and Antonia,[10] and Robinson[11] had also suggested the existence of a hierarchy of organized structures.

Head and Bandyopadhyay later used flow visualization to study zero-pressure gradient boundary layers for Reynolds numbers (based on momentum thickness) ranging from 500 to 17,500.[12] They observed "hairpin" vortices throughout the boundary layer. These hairpin loops were inclined to the wall at a characteristic "eddy angle" of 40–50 deg. The structures spanned the whole boundary layer. Whereas most of the research in this area had been dedicated to the study of incompressible flow, Robinson observed structures in supersonic flow which were similar to those found in incompressible flows.[11] Recent studies by Spina and Smits indicated the existence of organized structures in a zero-pressure gradient, supersonic, turbulent boundary layer.[2] In their investigation, small angles were measured near the floor; however, the angles increased to approximately 45 deg and remained constant throughout 70% of the boundary layer. The angle tended toward 90 deg near the outer edge of the boundary layer. Similar results were obtained in studies of organized structures of a supersonic boundary layer subjected to short regions of concave surface curvature by Donovan and Smits.[13] Perturbations of the flowfield tended to increase the inclination of the structure angle near the wall. In the present study, the existence of

Received Sept. 15, 1988; revision received Aug. 8, 1989.

*Graduate Research Assistant, Department of Mechanical Engineering.
†Associate Professor, Department of Mechanical Engineering. Senior Member AIAA.
‡Assistant Professor, Department of Aerospace and Ocean Engineering. Member AIAA.
§W. Martin Johnson Professor and Department Head, Department of Aerospace and Ocean Engineering. Fellow AIAA.

organized structures in a supersonic, slot-injected flowfield was investigated.

This paper first describes experimental background and techniques, and the measurements of organized structures in a turbulent boundary layer upstream of the slot injection flow. These are also compared with available published data. Results are then presented for the supersonic slot-injected flowfield at three stations downstream from the injector exit at distances corresponding to 4, 10, and 20 times the slot height. Reduced data showing average organized structure angle and integral length scale of turbulence are presented. Comparison of the changes in the flowfield characteristics between the baseline and with a weak oblique shock interacting with the mixing layer is described, ending with a general discussion and summary.

Experimental Background

The experiments were performed in the Virginia Tech 23 by 23 cm, "blow-down," supersonic wind tunnel. The setup consisted of a tangential supersonic slot injection into a supersonic stream. Both streams were air at about the same stagnation temperature. The model used had a slot height (1.27 cm), which was approximately the boundary-layer thickness in the primary stream and a thin splitter plate (0.52 mm). The wind tunnel was equipped with a Mach 3 nozzle block and a rearward facing step slot injector located under the centerline of the nozzle block. A sketch of the tunnel test section is presented in Fig. 1. The injector flow consisted of a supersonic nozzle Mach number of 1.7 at a total pressure of 73.8×10^3 N/m^2. The settling chamber pressure was maintained at 655.0×10^3 N/m^2 $\pm 0.3\%$ for the duration of the experiment. The mainstream unit Reynolds number was Re/cm = 5.4×10^5. Since the supersonic facility was a blow-down type, the duration of each run was less than 10 s. The stagnation temperature (nominally at 270 K) also decreased approximately 5°C during the run. Further details on the experimental setup are given in Ref. 1.

A nanoshadowgraph of the flowfield is presented in Fig. 2. The flow was from left to right. As can be seen, the flowfield consisted of the slot injection boundary layer near the floor of the test section, the slot injection freestream, a mixing region, and the tunnel freestream. The turbulent boundary-layer thickness (δ) on the wall approaching the slot was approximately 1 cm ($\delta/H = 0.8$). As can be seen from the photograph, the injected flow was slightly overexpanded. An adjustment shock and its reflection in the injectant stream can be seen just after the slot. The shear layer deflected toward the wall initially indicating a slightly overexpanded injection condition. The "lip" shock can be seen propagating into the freestream. From Fig. 2, evidence of large-scale structures can be seen in the shear layer that appeared to be slanted at a roughly 45 deg angle. Four stations are noted at the floor of the model. Measurements were obtained at X/H of -1, 4, 10, and 20, respectively. The origin of the axial coordinate (X) was located at the exit of the injector with the downstream direction being positive. Thus the first station ($X/H = -1$) corresponded to 1.27 cm upstream of the trailing edge of the splitter plate. Results obtained at $X/H = -1$ were compared with previously published data[2] as a consistency check.

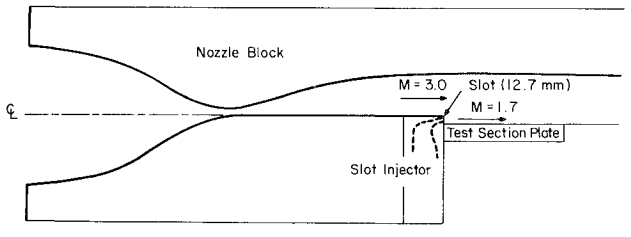

Fig. 1 Schematic of the wind tunnel arrangement (see Ref. 1).

From Fig. 2, effects of the lip shock as well as the adjustment shock can be seen at $X/H = 4$. The tunnel freestream, the mixing region, the slot injection freestream, and the lower wall boundary layer were all distinct at this station. Although not presented in this paper, a spark-Schlieren picture and mean Mach number profile showed that at $X/H = 10$, the shear layer and the lower wall boundary layer had not yet grown together, and a freestream of the slot flow can still be identified.[1] The shear layer and the lower wall boundary layer were found to merge at $X/H = 20$.

For clarity, the boundary layer on the mainstream side of the splitter plate upstream of the slot injector is referred to as the "upstream boundary layer." The shear layer (or mixing layer), which begins at X/H of 0, consists of the wake of the splitter plate and also the "outer shear layer." The outer shear layer is dominated by the upstream boundary layer shed from the splitter plate. In addition, there is a "lower wall boundary layer" on the floor of the tunnel.

Detailed measurements of the flowfield at the previously mentioned stations had been made with pitot and cone-static probes to determine mean profiles. The two dimensionality of the flowfield was also checked. Further details on the description of the flowfield can be found in Ref. 1.

Two cases were studied in this experiment—a basic slot injection configuration as described above (baseline) and the same case but with a deliberately produced shock wave impinging on the mixing zone to produce a sizable streamwise pressure gradient. The intent is to use these data in the future to investigate some of the terms in the Favre-averaged Turbulent Kinetic Energy (TKE) equation.[1]

Experimental Techniques

Measurements of Large-Scale Structure Angle

The thrust of the experiments was to determine if organized structures existed in the flowfield and if so, the corresponding structure angles. A parallel array dual-wire probe (DANTEC Model 55P71) with a fixed separation distance between hot wires of 1.33 mm (10% of the slot height) was used. The hot wires were made of platinum-plated tungsten wires of 5-μm diam and 1.25-mm length. The dual-wire probe was connected to two separate constant temperature anemometers (DISA 55D01) and operated at the same overheat ratio of 1.8. In

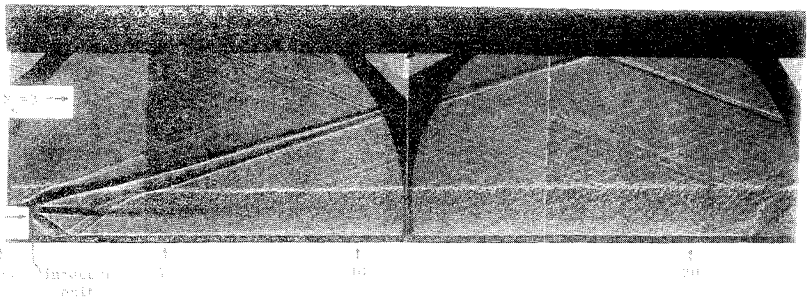

Fig. 2 Nanoshadowgraph of flowfield (see Ref. 1).

order to get high-frequency response, the bridge ratio of the anemometer was set at 1:1. The frequency response of the hot wires, as determined from a sine wave test, was approximately 160 kHz.[14] Phase shifts between signals must be avoided to obtain accurate correlation measurements. The hot-wire anemometers and signal conditioners were all identical, and the wires were only used if they had similar frequency response. All wires were checked for strain-gaging, and those found to be suspect were discarded.

For a given wire separation distance (w) a structure passing the parallel wire probe at a given angle will cause a time delay between the output of the hot wires. The time delay (τ) between the data resulting from the two hot-wire signals was obtained by performing a cross-correlation of the two signals. If this time delay is multiplied by the local mean velocity (U), the structure angle associated with an average large-scale motion can then be calculated as follows:

$$\theta = \tan^{-1}\left[\frac{w}{U\tau}\right]$$

The angle θ may be called an "average structure angle," in that it is associated with an average large-scale motion. Strictly speaking, the local streamwise convection velocity should be used to determine this angle, but the convection velocity has not been determined for this flow. However, the difference in the mean structure angle owing to variations in the convection velocity is small, and therefore the local mean velocity was used here. For example, if the local mean velocity changes by as much as 20%, the corresponding change in the mean structure angle is no more than 4 deg.

Two types of data acquisition systems were used in the experiments. The signals from the hot wires were recorded with a high-speed data acquisition system (LeCroy Model 6810 waveform recorder). The sample rate was 2 MHz. Fixed point measurements were taken for the large-scale structure angle, and 32,768 samples were obtained per hot-wire channel for each measurement. Given a wire separation distance of 1.33 mm, the high sampling rate (2 MHz) was required to resolve the average angle of the organized structure in this flowfield. Since calculation of average structure angles is dependent upon the time delay between the two hot-wire signals, tests were conducted using a signal generator to make sure that there was no inherent time delay between recording channels of the data acquisition system. Antialiasing filters were employed to prevent high-frequency content from folding back into the data.

Other low-frequency data such as probe position, total temperature, and pressure in the settling chamber, were recorded with a low-speed A/D board (Metrabyte) sampling at 1 kHz. The board interfaced with an IBM personal computer (PC), which was also used to control the operation of the tunnel.

Measurements of Integral Length Scale

The hot-wire data that were used to determine the structure angles were also analyzed to determine the integral length scale of turbulence. The autocorrelation function of the hot-wire signal was calculated, and the function was integrated over time to provide the integral time scale. By using Taylor's hypothesis, the integral time scale is multiplied by the local mean velocity, a characteristic length of the structure of the turbulence in the flow can be obtained.[15,16] The integral length scale in the streamwise direction cannot be measured by any intrusive probe (such as a hot-wire anemometer) in a supersonic flow. Although it is known that Taylor's approximation is not accurate in a shear layer,[17] it provides the only method available in the present study to estimate—however roughly—the turbulent length scale in the streamwise direction. For comparison purposes, integral time scales are valid measures which do not depend upon Taylor's approximation but may be related to integral length scales only in so far as Taylor's approximation is true.

It should be pointed out that due to the limit of the frequency response of the anemometer, turbulence length scale less than 3 mm cannot be resolved. Thus, all the length scale data presented in this paper are limited to 3 mm, even though the flowfield may contain length scales that are of smaller size.

Effect of Oblique Shock Interaction

The above measurements for large-scale structure angle and integral length scale were first obtained for the baseline. Then similar measurements were taken to investigate the effect of a shock impingement upon the shear layer. An oblique shock, generated on the upper wall of the tunnel with a wedge, impinged on the outer edge of the mixing layer at $X/H \approx 15$. The shock had a nominal pressure ratio of 1.82, which did not result in separation of the wall boundary layer. The profile distortion caused by this shock/viscous layer interaction on the large-scale structure angle and integral length scale was also documented and compared to the baseline.

Experimental Results

Large-Scale Structure Angle

Measurements were taken with the dual-wire probe in the upstream turbulent boundary layer. A typical trace of the fluctuating signal plotted against nondimensional time is presented in Fig. 3. The dimensionless time is defined as $U_\infty t/\delta$, where U_∞ is the freestream velocity, t is time, and δ is the thickness of the boundary layer. (For measurements upstream of the splitter plate, the boundary layer thickness of 1 cm is chosen as the nondimensional parameter as opposed to using the slot height.) Regions of the trace exhibiting similar characteristics indicate the passage of an organized structure larger than the wire separation distance. A nondimensional time shift between the two signals is apparent with the upper trace (hot wire #1) leading the lower trace (hot wire #2).

The cross correlations obtained at five locations are presented with respect to position in the boundary layer (Y/δ) in Fig. 4. The cross-correlation functions are plotted against nondimensional time. (For the streamwise station upstream of the splitter plate, the Y distance is measured from the top of the splitter plate up. Values of the cross correlation reach a high of 0.68 in the middle of the boundary layer decreasing only to 0.42 at the edge of the boundary layer. The nondimensional time delay between signals decreases from 1.8 in the middle of the boundary layer to nearly zero at the edge of the boundary layer. The highly correlated output coupled with the nonzero time delay indicates that both wires are detecting the same organized motion. A positive time shift in Fig. 4 indicates a structure inclining downstream.

Results of the average structure angle from measurements taken in the upstream boundary layer are presented in Fig. 5. The present data are represented as solid circles with the Y/δ locations corresponding to the center of the two hot wires. Data from Spina and Smits are presented as the shaded area.[2] The present data show that the angle is between 42 and 55 deg throughout the majority of the boundary layer. Although not shown in Fig. 5, the structure angle measured in the present study is found to increase to 90 deg at the edge of the boundary layer. Small angles were not detected near the floor; however, measurements could not be taken close enough to the floor with respect to the boundary layer thickness. The boundary layer studied was relatively small compared to boundary layers previously studied by Spina and Smits[2] making near-wall measurements difficult. Also the measurements reported in Ref. 2 were made on a zero pressure gradient turbulent boundary layer; whereas the present measurements were made in a turbulent boundary layer that was not necessarily in a zero pressure gradient. Despite this fact, Fig. 5 indicates the results of the present investigation show a similar trend compared to that of Ref. 2, establishing the consistency of the experimental procedure.

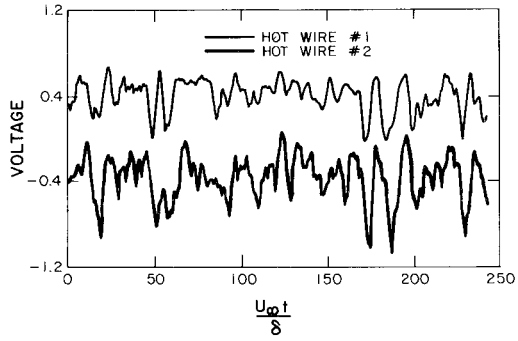

Fig. 3 Typical traces from two hot wires showing similarity between the signals.

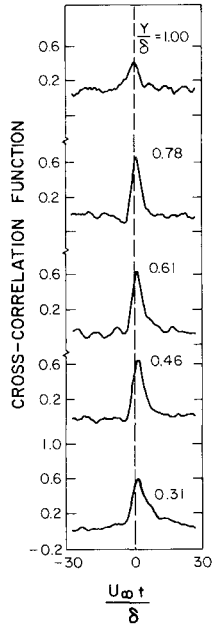

Fig. 4 The space-time correlation of hot-wire fluctuations throughout the boundary layer.

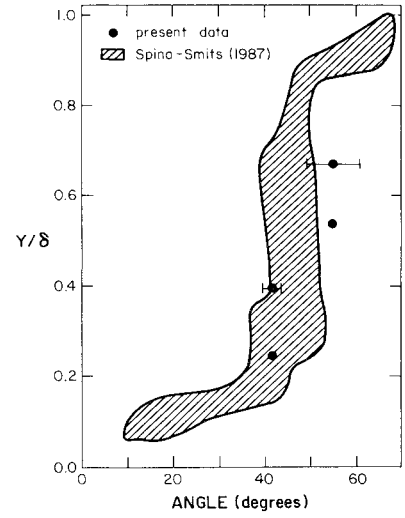

Fig. 5 Computed large-scale structure angle throughout the upstream boundary layer and comparison with data reproduced from Spina and Smits.[2]

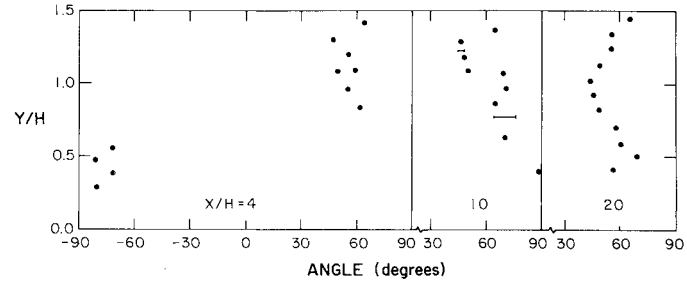

Fig. 6 Computed large-scale structure angle through the shear layer.

To determine an arithmetic mean and corresponding uncertainty for the time delay between signals, six measurements were taken in the middle of the boundary layer at the same fixed point. The arithmetic mean of the correlation was 0.66, and the uncertainty was 0.02. The arithmetic mean of the time delay was 5.8 μs with an uncertainty of 0.4 μs. To establish confidence intervals for probe location and structure angle, a statistical approach for describing uncertainties in single-sample experiments was taken.[18] Results indicate that the probe location lies within a confidence interval of ± 0.01 cm. The structure angles obtained lie within a confidence interval of ± 2 deg for an angle of about 45 and ± 6 deg for an angle of about 70 deg. The limitation here is due to the resolution of the time shift based on the digit count of the high-speed data acquisition system. The uncertainties are indicated in Fig. 5 as well as in subsequent figures.

In the upstream boundary layer study, the peak value of the cross correlation and the nonzero value of the time delay implied the existence of an organized structure. The correlation was relatively high throughout the boundary layer indicating the existence of an organized structure. For the slot-injected flowfield, regions of the flowfield are substantially different. One hot wire may be in the slot freestream, and the other wire may be in the boundary layer and thus regions of low correlation or no correlation were expected. A means of determining if an organized structure existed was necessary. Each data set was screened to determine if an organized structure passed the hot wires. First, the fluctuating time-dependent signals were analyzed. The peak-to-peak fluctuations of each hot wire were compared to determine if the hot wires were in the same region of the flowfield. Then the traces were further compared to determine if any common fluctuations were present. The final means of screening data were based on results from the cross-correlation. In general, cross correlations with peak values of 0.3 and less were rejected. The peak value of the cross correlation was difficult to determine for data sets exhibiting poor correlation.

Fixed point measurements of the average structure angle were taken at each station from the floor of the test section to the freestream. The flowfield was studied in detail at X/H of 4, 10, and 20. Results of the measurements for the average structure angle are presented in Fig. 6 in which the nondimensional vertical distance is plotted against average structure angle in degrees for all three stations. Beyond Y/H of 1.5, most of the data had a peak value of the cross correlation less than 0.3, and hence they were rejected. The velocity profiles, as inferred from other conventional steady-state instruments, are presented in Fig. 7.

At X/H of 4, Fig. 6 shows an abrupt transition occurs in the calculated average structure angles. Between Y/H of 0.3 and Y/H of 0.6, the average structure angles are seen to vary from -72 to -81 deg. Above Y/H of 0.6, the structure angles are on the order of 55 deg. The existence of a negative structure angle is not surprising considering the thin boundary layer developed on the underside of splitter plate in the injector. At a downstream station of $X/H = 4$, this boundary layer may not have completely mixed out. This argument is supported by the velocity profile presented in Fig. 7. An "inverted" boundary layer velocity profile is found to exist near Y/H of 0.6.

The results of the measurements at X/H of 4 can be visualized as being divided into two regions. The region above Y/H

of 0.7 is dominated by the upstream boundary layer. Comparing the results at X/H of 4 in Fig. 6 with the measurements upstream of the splitter plate in Fig. 5, it can be seen that the characteristic angle of 55 deg in the upper portion of the upstream boundary layer ($Y/\delta > 0.5$) still retains its identity at X/H of 4. At X/H of 4, the region of this 55 deg structure angle is extended to below Y/H of 1 (trailing edge of the splitter plate) and can be found even at Y/H of 0.7. The structure angle of 42 deg in the lower portion of the upstream boundary layer ($Y/\delta < 0.4$) in Fig. 5 cannot be identified in Fig. 6 at X/H of 4. It should be noticed from Fig. 7 that the wake of the splitter plate, as indicated in the velocity profile at X/H of 4, is not at Y/H of 1 but deflected downward at Y/H of 0.7. This is consistent with the nanoshadowgraph of the flowfield (see Fig. 2) showing the shear layer deflects toward the wall due to a slightly overexpanded injection condition. At X/H of 4, the lower wall boundary layer originated from the injector was still very thin. Measurements could not be taken close enough to the floor of the tunnel to identify this boundary layer.

Results of the measurements for the structure angle and velocity profile at X/H of 10 are also presented in Figs. 6 and 7. Again measurements were not taken close enough to the floor of the tunnel to identify the lower wall boundary layer. From the velocity profile in Fig. 7, it can be seen that a region dominated by the upstream boundary layer is still clearly visible between Y/H of 1.5 to 0.7. However, the wake of the splitter plate is now less distinguishable. Below Y/H of 0.4,

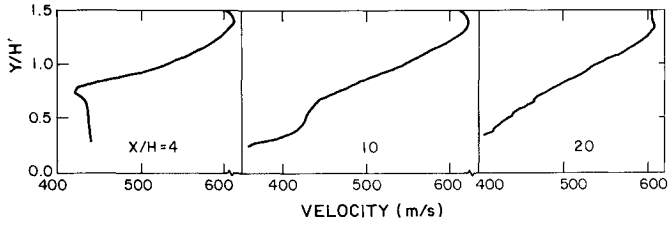

Fig. 7 Velocity profile inferred from steady-state measurements.

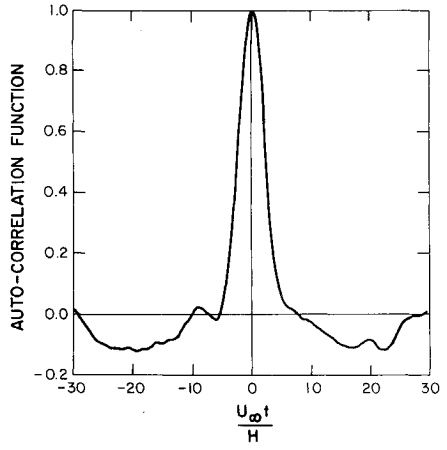

Fig. 8 Typical autocorrelation of hot-wire fluctuations.

the presence of the bottom boundary layer can also be seen on the velocity profile. At X/H of 10, the large-scale structure angle presented in Fig. 6 follows a similar trend as the velocity profile. The region between Y/H of 1.5 to 0.7 appears to be the remnant of the structure angles measured at X/H of 4, except the profile appears to be stretched in the vertical direction. The mean structure angle in this region is about 55 deg. Below Y/H of 0.6, the presence of the freestream of the slot is indicated by an increase of the structure angle to 70 deg as well as 88 deg. Notice the negative structure angle at X/H of 4 cannot be found at this axial station. This is not surprising since the boundary layer developed on the underside of the splitter plate in the injector is very thin, and by the time it gets to 10 slot heights downstream, it could be completely merged with the outer shear layer. This argument is also supported by the velocity profile in Fig. 7 in which the characteristic inverted boundary layer at X/H of 4 is not found at X/H of 10.

Results corresponding to 20 slot heights from the slot injector exit are also presented in Figs. 6 and 7. From spark-Schlieren flow visualization,[1] it can be seen at this streamwise station that the shear layer and the wall boundary layer have just started to merge. The velocity profile in Fig. 7 has begun to take on more of the appearance of a single boundary layer. However, the smooth velocity profile shown in Fig. 7 at this streamwise station does not necessarily imply that the average structure angle will follow the same smooth trend. The large-scale structures at this station are the result of the merging of two different large-scale structures. Those on the outer shear layer may still be dominated by the upstream boundary layer from the splitter plate. A mean structure angle of 55 deg in this region ($Y/H > 0.7$) can be seen in Fig. 6, in agreement with the mean angle in similar regions at X/H of 4 and 10 as well as the upstream station. The lower portion of the flowfield ($Y/H < 0.7$) may be dominated by the mixing of the shear layer with the upper portion of the boundary layer developed on the floor of the tunnel. Although the velocity profile seems to suggest a mix-out region at X/H of 20 (see Fig. 7), the nanoshadowgraph (see Fig. 2) clearly indicates that distinguishable flow features can still be identified between the outer shear layer and the lower wall boundary layer. The average structure angle at this station also supports this argument. From Fig. 6, the structure angle is seen to increase from 55 to about 65 deg in the lower portion of the shear layer.

Integral Length Scale

Figure 8 shows a typical autocorrelation function of the hot-wire fluctuations at a single location in the flow. Results of the integral length scale are summarized in Fig. 9 for all three stations. It must be emphasized again that a length scale of 3 mm or less cannot be resolved with the current hot-wire anemometer. Although not presented in Fig. 9, it was found that integral length scale of the order of 3 mm or less dominated the boundary layer upstream of the slot injection. From Fig. 9, at X/H of 4, it can be seen that above the wake of the splitter plate ($Y/H > 0.7$), the characteristic length scale is still on the order of 3 mm or less. At this station, the lower portion of the flowfield ($Y/H < 0.7$) shows integral length scales that scatter around 5 to 20 mm. Large variations in length scale can

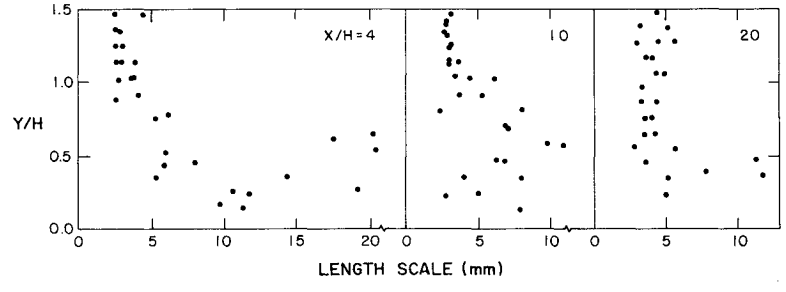

Fig. 9 Distribution of the integral length scale in the shear layer.

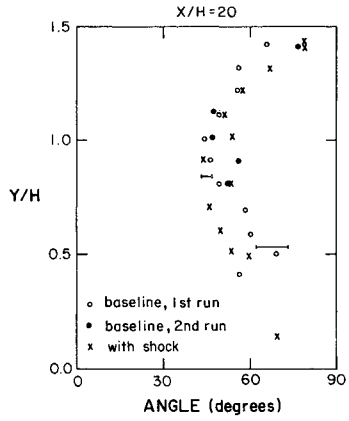

Fig. 10 Comparison between baseline and shock impingement for the large-scale structure angle.

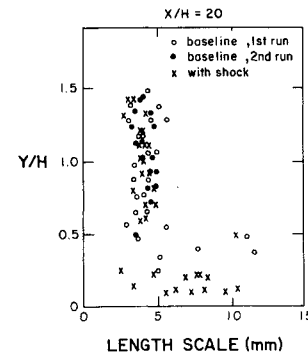

Fig. 11 Comparison between baseline and shock impingement for the integral length scale.

be seen at the same Y/H location. This is not surprising considering the fact that this region represents the freestream of the slot, and the intermittency at the lower edge of the shear layer and at the edge of the lower wall boundary layer may account for the variation in length scale. The integral time scale was obtained by integrating the autocorrelation function of 32,768 data points. (At a sampling rate of 2 MHz, this represents a duration of about 16 ms.) It was found that results were relatively independent of the number of data points used in the integration up to the limit of 32,768.

At $X/H = 10$, the outer shear layer remains unchanged compared to the previous station at X/H of 4. The integral length scale is relatively uniform and centers around 3 mm or less. However, the lower portion of the flowfield ($Y/H < 0.8$) experiences some modification; the variation in the length scale is now between 5 and 10 mm, and length scales greater than 10 mm do not exist anymore.

At a downstream distance of 20 slot heights, the overall distribution of the integral length scale changed considerably. Throughout the shear layer, the characteristic length scale is about 4 mm, an increase of 30% compared to the outer shear layer at the previous stations. In addition, the scatter in the lower portion of shear layer is reduced with very few data points showing length scale of 5 mm or more.

Comparison between Baseline and Shock Impingement

Results showing the comparison for the large-scale structure angle between baseline and with a weak oblique shock impinging on the shear layer are presented in Fig. 10. Measurements were taken at X/H of 20, about 5 slot heights downstream from where the oblique shock impinges on the top of the shear layer. Three data sets are presented. Two different series of runs were made for the baseline case to check repeatability. The data are presented as open circles for the first run and as solid circles for the second run, both for the baseline case. The data for the first run (open circle) are identical to those presented in Fig. 6. It can be seen that the measurements of the large-scale structure angle are repeatable to within experimental uncertainty. The data for the shock impingement case are presented as x in Fig. 10. Within experimental accuracy, no measurable difference is found in the large-scale structure angle for the baseline and the shock impingement case.

Figure 11 shows the comparison for the integral length scale between baseline and shock impingement. The data for the first run (open circle) are identical to those presented in Fig. 9. It can be seen from Fig. 11 that the data are repeatable between the first and second runs and that no significant change is observed in the integral length scale due to the impingement of the oblique shock. Figure 11 also shows that there is a lot of scatter in the data near the floor of the tunnel between Y/H of 0.1 and 0.5. The reason for this is not known yet, but perhaps it is caused by the intermittency at the edge of the lower wall boundary layer since at this streamwise station, there is evidence that the lower wall boundary layer has not yet been completely mixed with the shear layer. Most of the data below Y/H of 0.4 in Fig. 11 do not have a high enough cross-correlation coefficient to be accepted for the determination of the large-scale structure angle, and hence those data are not presented in Fig. 10.

Discussion

There is a possibility that a Karman vortex street may exist in the flowfield due to the presence of the rearward facing step of the injector as well as the splitter plate. The appropriate length scales for the vortex shedding would be the thickness of the upstream boundary layer (1.0 cm) and the thickness of the splitter plate (0.52 mm). The corresponding vortex shedding frequencies, based on a Strouhal's number of 0.2, were estimated to be 10 and 200 kHz, respectively. Fast Fourier transforms of the hot-wire data do not reveal the presence of any predominant frequency. Furthermore, there is no evidence of a vortex roll-up structure that should be visible on the nanoshadowgraphs. Thus it is unlikely that a vortex street can be found to exist in the studied shear layer.

The average structure angle measurements reported here are useful in describing the overall large-scale structure of the shear layer. No attempt was made to measure instantaneous behavior in this experiment. However, results from Spina and Smits[2] had shown that for a zero pressure gradient turbulent boundary layer, the average value of the instantaneous angle matched the mean structure angle very well. The overall trend of the measurements reported here shows a structure angle of about 55 deg in most of the shear layer. At the edge of the shear layer, the angle tends toward 90 deg. These trends can be interpreted in terms of the hairpin model of wall turbulence. In this model, the characteristic structures in the boundary layer are hairpin loops, and hairpins of all sizes populate the boundary layer. A typical hairpin vortex consists of elongated legs at the floor inclined at a small angle (20 deg), a central portion inclined at 45 deg, and an upturned head at 90 deg.[12] The deduced structure angles from this investigation are consistent with this model. Based on the results presented here, it may be postulated that the lower leg of the hairpin vortex quickly loses its identity once it is ejected from the wall and then convected downstream from the trailing edge of the splitter plate. The upper shear layer then appears to be the remnants of structures observed in the central portion of the upstream boundary layer with a characteristic incline angle of 55 deg. There is one important implication from the present experiment: in the slot injection flowfield, once a hairpin vortex is shed from the splitter plate and convected downstream, there is no nearby wall to continue to feed hairpin vortices into the shear layer. This experimental investigation found that large-scale structures, originated from the upstream boundary layer, seem to retain much of their shape and character as they convect downstream in a compressible shear layer. It appears

that they preserve their identity for as much as 20 slot heights downstream (about 25 times the upstream boundary layer thickness) from where they leave the solid wall of the splitter plate. In addition, by comparing the profiles of the structure angle at all three stations in Fig. 6, the data appear to support the idea that the structures are stretched vertically and pulled downward toward the tunnel floor as they are convected downstream, perhaps due to the overexpanded injection condition. However, at this stage the suggestion can only be considered as conjectural, and further experimental studies are needed to verify this.

Conclusions

Leaving aside the more speculative aspects of the preceding discussion, the conclusions of the present investigation may be summarized as follows. The behavior of the average large-scale structure in a supersonic flow with supersonic slot injection was studied using a parallel array, constant temperature, dual-wire probe. To determine if the experimental procedure for obtaining the average structure angle of the organized motions was consistent with previous studies, a turbulent boundary layer generated on the upper side of the splitter plate upstream of the slot injector was studied. Results were consistent with published data, i.e., a structure angle on the order of 55 deg was seen to dominate the majority of the boundary layer. After determining consistency of the experimental technique, the supersonic flow with supersonic slot injection was studied. Large-scale structure angles obtained at each station resulted in distinct regions describing the flowfield. Of particular interest was a region ranging from approximately Y/H of 0.7 to 1.5. Structures in this region appeared to be the remnants of structures observed in the boundary layer, which developed on the upper side of the splitter plate prior to the supersonic slot injection. Large-scale structure angles on the order of 55 deg were measured in this region. At station X/H of 20, the shear layer was seen to merge with the thin boundary layer developed on the floor of the tunnel from the supersonic slot injection.

Characteristic length scales of turbulence were also obtained based on the integral time scales calculated from the autocorrelation functions of the hot-wire signals and the use of Taylor's hypothesis. Length scales of 3 mm or less dominated the turbulent boundary layer upstream of the slot injection as well as the outer portion of the shear layer at X/H of 4 and 10. At X/H of 20, the length scales increase to 4 mm in the outer portion of the shear layer.

After studying the unperturbed flowfield (baseline), the effect of a weak oblique shock impinging on the shear layer at X/H of 15 was studied. Measurements were repeated at X/H of 20 to determine the effect of the pressure gradient on the flowfield. Large-scale structure angles as well as integral length scale appeared relatively unaffected by the streamwise pressure gradient.

Acknowledgments

This work was supported by the Applied Physics Laboratory of the Johns Hopkins University, Harold E. Gilreath, Contract Monitor. Additional support also came from the Hypersonic Propulsion Branch at NASA Langley Research Center, Griffin Y. Anderson, Branch Chief. The authors are indebted to Randy Hyde and Ben Smith for obtaining the mean velocity profiles presented in Fig. 7.

References

[1]Walker, D. A., Campbell, R. L., and Schetz, J. A., "Turbulence Measurements for Slot Injection in Supersonic Flow," AIAA Paper 88-0723, Jan. 1988.

[2]Spina, E. F., and Smits, A. J., "Organized Structures in a Compressible, Turbulent Boundary Layer," *Journal of Fluid Mechanics,* Vol. 182, No. 1, 1987, pp. 85-109.

[3]Kline, S. J., Reynolds, W. C., Schraub, F. A., and Runstadler, P. W., "The Structure of Turbulent Boundary Layer," *Journal of Fluid Mechanics,* Vol. 30, No. 4, 1967, pp. 741-773.

[4]Corino, E. R., and Brodkey, R. S., "A Visual Investigation of the Wall Region in Turbulent Flow," *Journal of Fluid Mechanics,* Vol. 37, No. 1, 1969, pp. 1-3.

[5]Kim, T. H., Kline, S. J., and Reynolds, W. C., "The Production of Turbulence Near a Smooth Wall in a Turbulent Boundary Layer," *Journal of Fluid Mechanics,* Vol. 50, No. 1, 1971, pp. 133-160.

[6]Brown, G. L., and Thomas, A. S. W., "Large Structure in a Turbulent Boundary Layer," *Physics of Fluids,* Vol. 20, No. 10, 1977, pp. 243-252.

[7]Chen, C. P., and Blackwelder, R. F., "Large-Scale Motion in a Turbulent Boundary Layer: A Study Using Temperature Contamination," *Journal of Fluid Mechanics,* Vol. 89, No. 1, 1978, p. 131.

[8]Moin, P., and Kim, J., "The Structure of the Vorticity Field in Turbulent Channel Flow. Part 1—Analysis of Instantaneous Fields and Statistical Correlations," *Journal of Fluid Mechanics,* Vol. 155, No. 1, 1985, pp. 441-464.

[9]Thomas, A. S. W., and Bull, M. K., "On the Role of Wall-Pressure Fluctuations in Deterministic Motions in the Turbulent Boundary Layer," *Journal of Fluid Mechanics,* Vol. 128, No. 1, 1983, pp. 283-332.

[10]Rajagopalan, S., and Antonia, R. A., "Some Properties of the Large Scale Structure in a Fully Developed Turbulent Duct Flow," *Physics of Fluids,* Vol. 22, No. 4, 1979, pp. 614-630.

[11]Robinson, S. K., "Space-Time Correlation Measurements in a Compressible Turbulent Boundary Layer," AIAA Paper 86-1130, 1986.

[12]Head, M. R., and Bandyopadhyay, P., "New Aspects of Turbulent Boundary Layer Structure," *Journal of Fluid Mechanics,* Vol. 107, No. 1, 1981, pp. 297-338.

[13]Donovan, J. F., and Smits, A. J., "A Preliminary Investigation of Large-Scale Structure in a Fully Developed Turbulent Duct Flow," AIAA Paper 87-1285, June 1987.

[14]Walker, D. A., Ng, W. F., and Walker, M. D., "Experimental Comparison of Two Hot-Wire Techniques in Supersonic Flow," *AIAA Journal,* Vol. 27, No. 8, Aug. 1989, pp. 1074-1080.

[15]Schlichting, H., *Boundary-Layer Theory,* McGraw-Hill, New York, 7th ed., 1987, p. 568.

[16]Hinze, J. O., *Turbulence,* McGraw-Hill, New York, 2nd ed., 1987, p. 46.

[17]Owen, F. K., and Horstman, C. C., "On the Structure of Hypersonic Turbulent Boundary Layers," *Journal of Fluid Mechanics,* Vol. 53, No. 4, 1972, pp. 611-636.

[18]Kline, S. J., and McClintock, R. A., "Describing Uncertainties in Single-Sample Experiments," *Mechanical Engineering,* Jan. 1953, pp. 3-7.